Ikram Maaoui-Ben Hassine, Mohamed Wissem Naouar, Najiba Mrabet-Bellaaj

J. Electrical Systems 11-4 (2015): 463-475

Regular paper

Journal of Electrical Systems

Model Based Predictive Control For Three-Phase Grid Connected Converter

Model based Predictive Control (MPC) is an efficient control technique for the control of power converters. It has several advantages for this kind of controls, such as robustness to parameters variations and fast dynamic responses. The MPC considers the model of the converter-based system to forecast possible future behavior of the controlled variable. It allows selecting the optimal voltage vector to be applied so that a predefined cost function is minimized. This paper focuses on an MPC algorithm for three-phase grid connected converter. Several simulation results (under Matlab-Simulink software environment tool) and experimental results (under developed prototyping platform) are presented in order to show the effectiveness of the considered control strategy.

Keywords: Wind power generation, Three-phase grid connected converter, Model Predictive Control.

Article history: Received 15 December 2014, Received in revised form 30 September 2015, Accepted 19 October 2015

1. Introduction

During last years, Distributed Generations (DG) of electrical power integrating renewable energy sources are increasingly used because of their environmental and economic interest compared to traditional generators. Recently, distributed power generation based on wind energy has become one of the world's fastest growing energy sectors, helping to satisfy the global energy demands [1]-[2]-[3]. In grid connected wind energy systems, the three-phase grid connected converter play a key role to connect the wind energy generator to the utility grid. To achieve high control performances, several issues have been studied in the literature, including converter topologies, modulation strategies and control strategies [4]-[5]. For this reason, the development of high performance control strategies for three-phase grid connected converter becomes of prime importance, since it allows to meet standards and grid interconnection requirements [6]-[7]. The control scheme of a grid-connected converter is usually divided into three parts:

- Grid synchronization part: This part is generally used to compute the grid voltage position θ_{dq}. It is based on the use of Phase Locked Loop (PLL) [8] and is particularly aimed to synchronize the control with regard to the grid voltage vector.
- dc-link voltage control part: This part is generally aimed to control the dc-link voltage V_{dc} in the dc-side of the grid connected converter. In most cases, the control of the dc-link voltage is based on a simple PI controller.
- Current control part: This part is generally aimed to control the grid currents i_{gabc} in the grid side of the grid connected converter.

Corresponding author : Ikram Maaoui-Ben Hassine, email: ikram_m4@yahoo.fr
National school of Tunis, Tunisia, University of Tunis, Tunisia.

The current control part is the most important one to meet new grid codes specified by national standards for the connection of power converters to the grid. Moreover, it allows controlling the power flow through the converter, namely the active power P, the reactive power Q and in some cases the distorted power D. So, robust and efficient current control algorithms should be used in order to ensure required performances. To this purpose, several control strategies based on different current control algorithms have been studied and developed [9]-[10]. Among them, we can quote the Direct Power Control (DPC) [11] and the DPC-SVM [12]. For the DPC algorithm, the current control part is based on nonlinear hysteresis controllers associated to a switching table. For the DPC-SVM algorithm, the current control part is based on linear PI controllers associated to a Space Vector Modulation (SVM) process. Nowadays, a growing interest is also paid for Model Predictive Control (MPC) algorithms due to their robustness and performances [13]-[14]-[15]-[16]. During last decade, their implementation on digital solutions was limited by computation delays that affect the predictive control performances [17]. The recent revolution in digital electronic technologies allowed performing real time computation of predictive control algorithms despite their complexity. Compared to the DPC algorithm, MPC algorithms provide lower current THD with the same dynamic performances. Besides, they are characterized by a mean variable switching frequency lower than the case of the DPC algorithm. Compared to the DPC-SVM algorithms, MPC algorithms provide higher current THD with faster dynamic performances [18]. In addition, they are less sensitive to parameters variations.

This work is aimed to present an MPC algorithm used for the control of three-phase grid connected converter. The considered MPC algorithm is based on prediction and optimization tasks. The prediction task is performed based on the mathematical model of a three-phase grid connected converter, while the optimization one is performed based on a predefined cost function. During each sampling period, the optimal converter voltage vector is computed as follows. Firstly, the grid current trajectories are computed based on the mathematical model of the three-phase grid connected converter. These trajectories are computed for all switching signal combinations that lead to seven different converter voltage vectors. The optimization task is then achieved by selecting the switching signals combination that minimizes a cost function. This last is defined so that minimal error between the grid current reference vector and the predicted one is obtained [19]-[20]-[21]-[22]-[23].

This paper is organized as follows. In section II, the model of three-phase grid connected converter is firstly presented. Then, the MPC algorithm is detailed and discussed according to the obtained simulation results. Finally, section III presents numerous experimental results in order to show the effectiveness of the proposed MPC algorithm.

2. Three-phase grid connected converter model

The power circuit of a three-phase grid connected converter is presented in Fig.1. As depicted in this figure, an L filter is used to interface between the grid and the converter, where L_g denotes the inductor value and R_g its equivalent serial resistance.

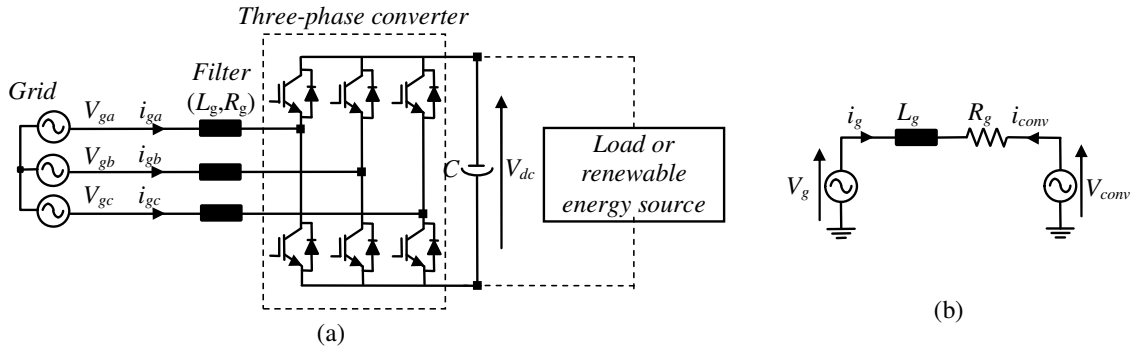

Fig.1. (a) Power circuit of the three-phase grid connected converter through *L* filter (b) Single phase equivalent circuit

$V_{gi,(i=a,b,c)}$ (respectively $i_{gi,(i=a,b,c)}$) refer to the grid voltage vector components (respectively the grid current vector components) in the stationary reference frame, while V_{dc} refer to the dc-link voltage. The mathematical model of the three-phase grid connected converter in the *dq* synchronous reference frame is characterized by the following equations.

$$\frac{di_{gd}}{dt} = \frac{1}{L_g}\left(V_{gd} - R_g i_{gd} + \omega_g L_g i_{gq} - V_{convd}\right) \quad (1)$$

$$\frac{di_{gq}}{dt} = \frac{1}{L_g}\left(V_{gq} - R_g i_{gq} - \omega_g L_g i_{gd} - V_{convq}\right) \quad (2)$$

$$P = V_{gd} i_{gd} + V_{gq} i_{gq} \quad (3)$$

$$Q = V_{gq} i_{gd} - V_{gd} i_{gq} \quad (4)$$

Where di_{gd}/dt and di_{gq}/dt are the instantaneous grid current time derivatives. V_{gd} and V_{gq} (respectively i_{gd} and i_{gq}) are the *d* and *q* components of the grid voltage vector (respectively the grid current vector) and ω_g is the angular frequency of the grid voltage. V_{convd} and V_{convq} are the *d* and *q* components of the converter output voltage vector. L_g and R_g are respectively the resistor and inductor of the used *L* filters. Taking into account that the *d* axis is linked to the grid voltage vector (V_{gq}=0), equations (3) and (4) can be simplified as follows

$$P = V_{gd} i_{gd} \quad (5)$$

$$Q = -V_{gd} i_{gq} \quad (6)$$

3. Model based predictive control

The proposed MPC algorithm is based on the discrete system model, which is used to predict system response during the next sampling period [24]. The main objective of the MPC algorithm is to control the active and reactive power through the control of the *d* and *q* grid current components.

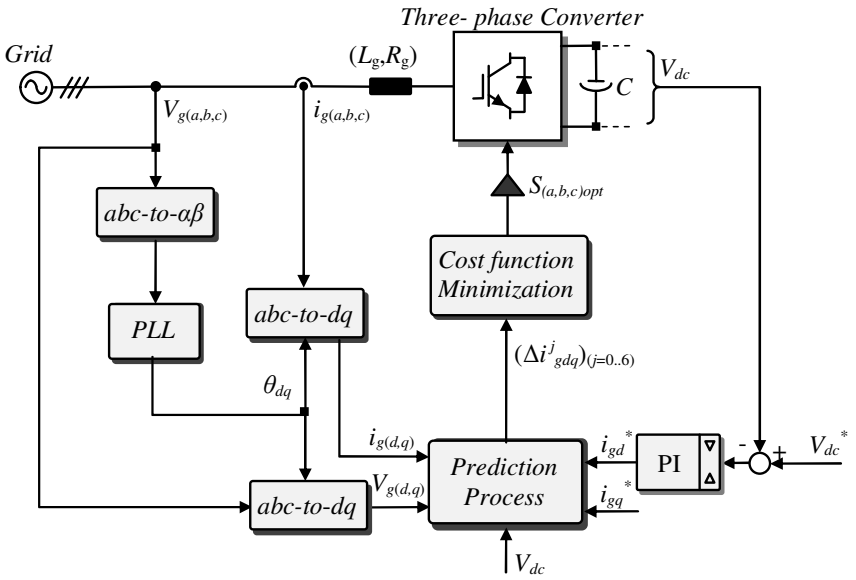

Fig.2. MPC-based control for three-phase grid connected converter

The MPC-based control for three-phase grid connected converter is presented on Fig.2. As shown in this figure, a cascade control structure is used. In one hand, a PI-based external control loop controls the dc-link voltage V_{dc}. On the other hand, an MPC-based internal control loop controls the grid currents in the *dq* synchronous reference frame, where the *d* axis is linked to the grid voltage vector. According to equations (1) and (2), and using the forward Euler discretization method, the digital prediction equations are deduced as in (7) and (8).

$$i_{gd}[k+1] = a_0\left(V_{gd}[k] - V_{convd}[k]\right) + a_1 i_{gd}[k] + a_2 i_{gq}[k] \tag{7}$$

$$i_{gq}[k+1] = a_0\left(V_{gq}[k] - V_{convq}[k]\right) + a_1 i_{gq}[k] - a_2 i_{gd}[k] \tag{8}$$

Where $a_0=T_s/L_g$, $a_1=(1-R_gT_s/L_g)$ and $a_2=\omega_g T_s$. T_s is the sampling period. $i_{gd}[k+1]$ and $i_{gq}[k+1]$ (respectively $i_{gd}[k]$ and $i_{gq}[k]$) are the predicted *d* and *q* grid current components at the $(k+1)^{th}$ sampling period (respectively measured *d* and *q* grid current components during the k^{th} sampling period).

During each sampling period, the evolution of the *d* and *q* grid current components depends on the applied converter voltage components $V_{convd}[k]$ and $V_{convq}[k]$ at the k^{th} sampling period. These voltage components used for the current prediction are expressed in the *dq* synchronous reference frame and can be determined through the application of a rotation operation (with an angle equal to θ_{dq}) to the $\alpha\beta$ components of the converter voltage vectors. The θ_{dq} position is the grid voltage vector position and is computed through a PLL. It should be noted that the voltage vectors $V^j_{convd}[k]$ and $V^j_{convq}[k]$ depend also on the dc-link voltage V_{dc} level as shown in equations (9) and (10). For simplification reasons, the dc-link voltage is assumed equal to its reference V_{dc}^*.

$$\begin{bmatrix} V^j_{convd}[k] \\ V^j_{convq}[k] \end{bmatrix} = \begin{bmatrix} \cos(\theta_{dq}[k]) & \sin(\theta_{dq}[k]) \\ -\sin(\theta_{dq}[k]) & \cos(\theta_{dq}[k]) \end{bmatrix} \begin{bmatrix} V^j_{conv\alpha}[k] \\ V^j_{conv\beta}[k] \end{bmatrix} \tag{9}$$

$$\begin{bmatrix} V^{j}_{conv\alpha}[k] \\ V^{j}_{conv\beta}[k] \end{bmatrix} = \frac{2}{3} V^{*}_{dc} \begin{bmatrix} 1 & -\frac{1}{2} & -\frac{1}{2} \\ 0 & \frac{\sqrt{3}}{2} & -\frac{\sqrt{3}}{2} \end{bmatrix} \begin{bmatrix} S_a[k] \\ S_b[k] \\ S_c[k] \end{bmatrix} \quad (10)$$

Where $V^{j}_{conv\alpha}[k]$ and $V^{j}_{conv\beta}[k]$ are the output converter voltage vectors in the stationary coordinates $\alpha\beta$, and $S_a[k]$, $S_b[k]$ and $S_c[k]$ are the switching signals for each phase of the converter.

Hence, to perform the prediction process, seven cases must be taken into account since the number of switching states combinations is equal to eight with two combinations that lead to null converter voltage vector as presented in equations (11) and (12), where $(i^{j}_{gd}[k+1])_{(j=0..6)}$ and $(i^{j}_{gq}[k+1])_{(j=0..6)}$ are the predicted d and q grid current components at the $(k+1)^{th}$ sampling period when the $(V^{j}_{conv\alpha}[k])_{(j=0..6)}$ and $(V^{j}_{conv\beta}[k])_{(j=0..6)}$ voltage vector components are applied during the k^{th} sampling period.

$$\left(i^{j}_{gd}[k+1] = a_0 \left[V_{gd}[k] - V^{j}_{convd}[k] \right] + a_1 i_{gd}[k] + a_2 i_{gq}[k] \right)_{(j=0..6)} \quad (11)$$

$$\left(i^{j}_{gq}[k+1] = a_0 \left[V_{gq}[k] - V^{j}_{convq}[k] \right] + a_1 i_{gq}[k] - a_2 i_{gd}[k] \right)_{(j=0..6)} \quad (12)$$

Table1: Converter switching states and corresponding output voltage vectors $\vec{V}^{j}_{convdq(j=0..6)}$

S_a	S_b	S_c	$V^{j}_{conv\alpha}$	$V^{j}_{conv\beta}$	$\vec{V}_j$	$\vec{V}^{j}_{convdq}$
0	0	0	0	0	V_0	V^{0}_{convdq}
1	0	0	$2V_{dc}/3$	0	V_1	V^{1}_{convdq}
1	1	0	$V_{dc}/3$	$V_{dc}/\sqrt{3}$	V_2	V^{2}_{convdq}
0	1	0	$-V_{dc}/3$	$V_{dc}/\sqrt{3}$	V_3	V^{3}_{convdq}
0	1	1	$-2V_{dc}/3$	0	V_4	V^{4}_{convdq}
0	0	1	$-V_{dc}/3$	$-V_{dc}/\sqrt{3}$	V_5	V^{5}_{convdq}
1	0	1	$V_{dc}/3$	$-V_{dc}/\sqrt{3}$	V_6	V^{6}_{convdq}
1	1	1	0	0	V_7	V^{7}_{convdq}

As mentioned previously, the MPC algorithm is aimed to achieve a minimum grid current error in the next sampling period. To this purpose, it is possible to firstly predict the dq grid current error vector components $(\vec{\Delta} i^{j}_{gd}[k+1])_{(j=0..6)}$ and $(\vec{\Delta} i^{j}_{gq}[k+1])_{(j=0..6)}$. These errors are defined as the difference between the reference grid current vector at the k^{th} sampling period and the predicted one at the next sampling period $(k+1)^{th}$ when the converter voltage vector $(\vec{V}^{j}_{convdq}[k])_{(j=0..6)}$ is applied. So, the grid current error vector components $(\vec{\Delta} i^{j}_{gd}[k+1])_{(j=0..6)}$ and $(\vec{\Delta} i^{j}_{gq}[k+1])_{(j=0..6)}$ are expressed as in (13) and (14).

$$(\Delta i^{j}_{gd}[k+1] = i^{*}_{gd}[k] - i^{j}_{gd}[k+1])_{(j=0..6)} \quad (13)$$

$$(\Delta i^{j}_{gq}[k+1] = i^{*}_{gq}[k] - i^{j}_{gq}[k+1])_{(j=0..6)} \quad (14)$$

Then, a cost function g is applied to the obtained grid current error components. This cost function is defined in equation (15).

$$(g^j = \left|\Delta i_{gd}^j[k+1]\right| + \left|\Delta i_{gq}^j[k+1]\right|)_{(j=0..6)} \quad (15)$$

The core of the predictive algorithm is the cost function minimization [13]-[14]. The optimal switching signals $S_{(a,b,c)}^{opt}$ that lead to the minimal cost function value $\text{Min}(g^j)_{(j=0..6)}$ are selected and applied to the converter. Note that for the case of null voltage vector, the selected $S_{(a,b,c)}^{opt}$ switching signals depend on the applied switching signals during the previous sampling period so that the switching frequency is reduced.

A set of simulation studies developed under Matlab-Simulink environment tool were performed in order to show the effectiveness of the proposed MPC-based control for three-phase grid connected converter. It should be noted that during simulation procedure, the following operation conditions were used:

- The dc-link capacitor was initially charged to 500V.
- The dc-link voltage reference V_{dc}^* was set to 600V.
- The q axis grid current reference i_{gq}^* was set equal to zero for unit power factor operation.

Also, it should be noted that simulation and experimental results, are presented only for the case where the grid connected converter works as three phases PWM boost rectifier. The achieved control is of course also available for the case when the converter works as a three-phase inverter.

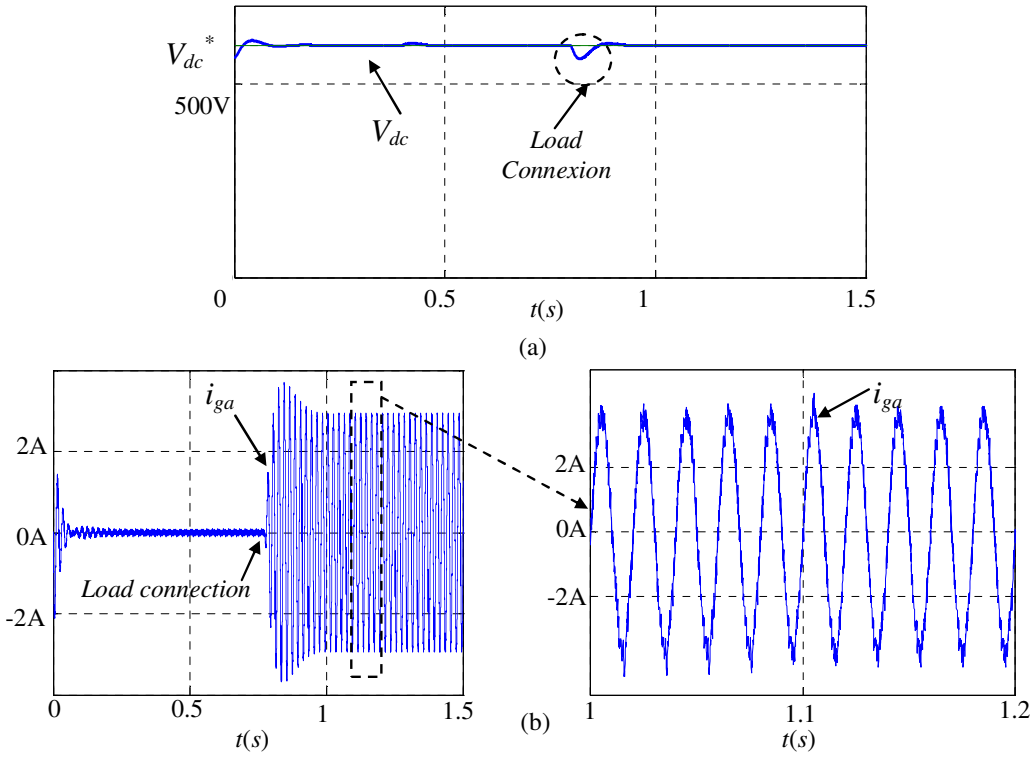

Fig.3. Response to a step reference of 600V applied to the reference dc-link voltage and load step change at 0.8s (a) dc-link voltage response
(b) Grid current response

Fig.3.a presents the response of the dc-link voltage to a step reference V_{dc}^* equal to 600V. The start-up of the MPC control was done at no load. Then, at 0.8s, a step load change was applied by connecting a resistive load to the DC side. The obtained simulation results show that during steady state operation, the error of the dc-link voltage V_{dc} becomes equal to zero. A small backward overshoot appears when the load is connected. Then, the PI

controller compensates the disturbance due to load connection. Fig.3.b shows the grid current i_{ga} response. It can be noted that i_{ga} increases when the load is connected and has a sinusoidal waveform. Fig.4 shows the waveform of the grid current i_{ga} with regard to the grid voltage V_{ga} during steady state operation. As expected, a unit power factor operation was achieved with a sinusoidal grid current absorption. The obtained THD for the grid current i_{ga} is equal to 7.8%.

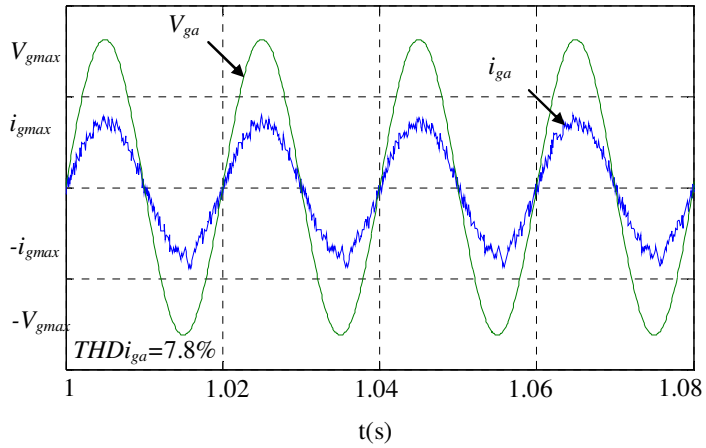

Fig.4. Grid voltage V_{ga} and current i_{ga} waveforms during steady state operation

Based on the simulation results of the MPC algorithm and the results presented in [18], we can deduce a comparison with other standard control algorithms as detailed in Table 2.

TABLE2: Comparison between performances of MPC algorithm and standard control algorithms

Criteria/ Control	**DPC**	**DPC-SVM**	**MPC**
Switching frequency	Variable	Constant	Variable
Current THD	10.8%	3.46%	7.8%
Robustness	+	-	+

These results demonstrate that the considered MPC algorithm achieves lower current THD than the DPC algorithm and faster dynamic performances than the DPC-SVM algorithm. In addition, it is less sensitive to parameters uncertainties.

4. Experimental set-up

In order to illustrate the performances of the MPC algorithm, experiments were carried out on a prototyping platform based on STM32F4 microcontroller that controls a three-phase PWM boost rectifier. This prototyping platform is presented in Fig.5 and includes two main parts:

The first one is a power part, which is composed of:

- The grid source
- A 20 kVA three-phase converter.
- An autotransformer is used to vary the voltage peak magnitude of the grid voltages in the grid side converter.
- Three *L* filters (50mH/20A) placed between the autotransformer and the converter.
- A dc-link capacitor (1100µF/800V).
- A variable resistive load connected to the dc-link capacitor.

The second one is a control part, which is composed of:

- Measurement board that provides current and voltage measurements.
- The STM32F4 microcontroller where the MPC-based algorithm was implemented. This microcontroller is based on Cortex-M4-ARM processor, which is associated to a Floating Point Unit (FPU) and works with system clock frequency equal to 168 MHz.
- An Interface board to adapt the voltage level between STM32F4 and the converter drivers.
- Host PC used to configure STM32F4 microcontroller.

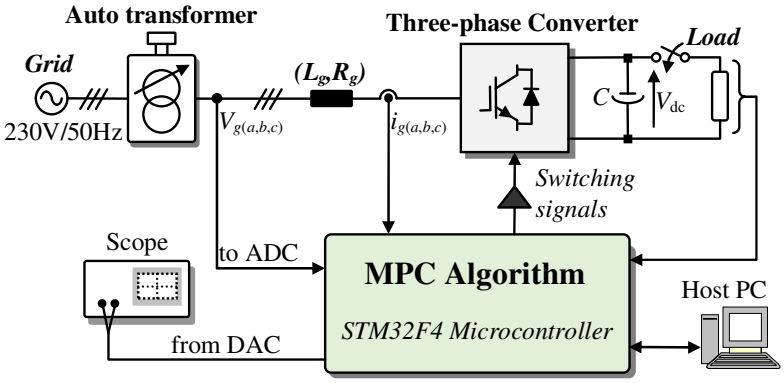

Fig.5. Prototyping platform

During experimentation, the following operation conditions were taken considered:
- The dc-link capacitor was initially charged by acting on the autotransformer to 150V.
- The dc-link voltage reference V_{dc}^{*} was set to 200V.

Fig.6. presents the timing diagram of the implemented control. This diagram presents the computation cycles of the different modules during each sampling period, where t_{PI} is the computation time of the PI controller and T_{MPC} is the computation time of the predictive controller. By adding the A/D conversion time, the whole execution time T_{ex} of the control architecture is equal to 114 μs. Taking into account the execution time T_{ex} of the MPC-based algorithm, the used sampling period T_s was set equal to 125μs. It can be noted that the switching states $S_{(a,b,c)opt}$ are refreshed every sampling period. However, the application of the switching states is not instantaneously, but after an execution time T_{ex}.

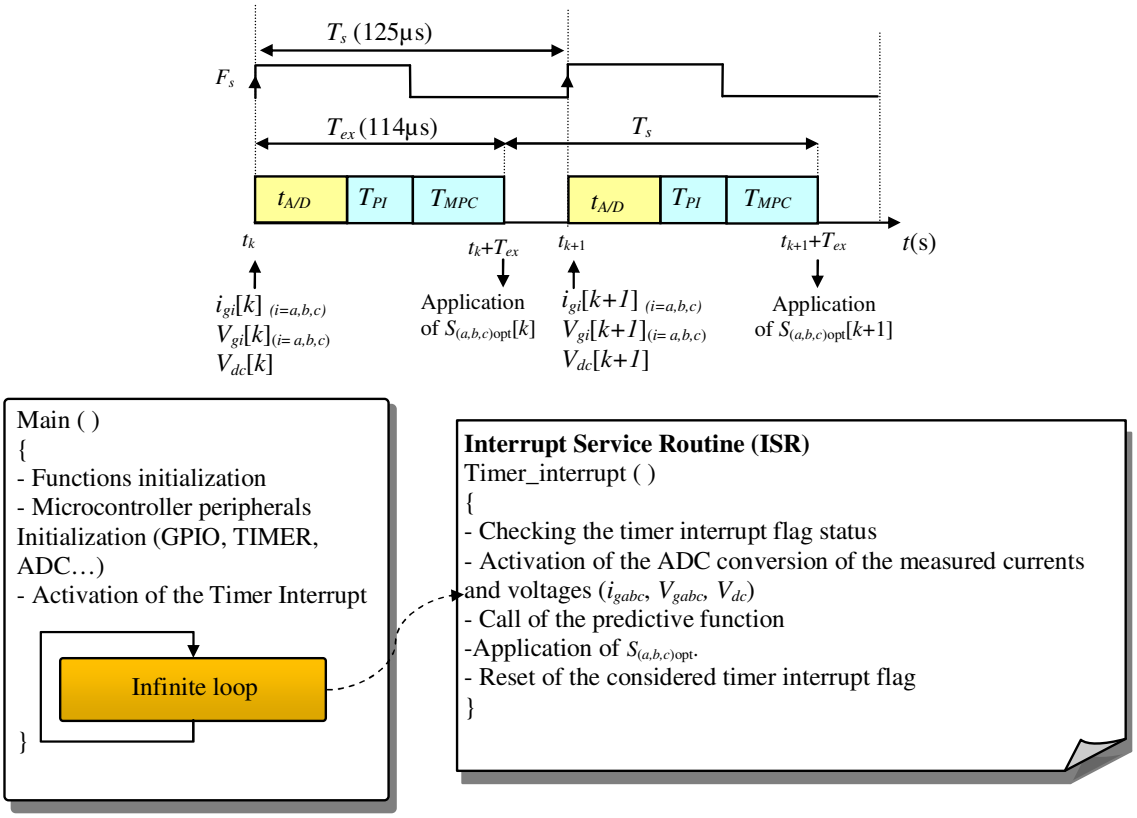

Fig.6. Timing diagram of the MPC-based algorithm

Table 2: Timing performances of the MPC-based algorithm

Module	Computation time
A/D conversion	$t_{A/D}$ **= 14.2µs**
PI	t_{PI}**=7.8µs**
MPC	t_{MPC}**= 92µs**
$Tex= t_{A/D} + t_{PI}+ t_{mpc}$ **=114µs**	

The obtained experimental results for the MPC algorithm are presented on Fig.7, Fig.8 and Fig.9. The experimental tests were achieved in three steps. In the first step, the switching signals of the three-phase converter were tied low and the load is disconnected. In this case, the converter works as a simple three-phase diode bridge rectifier. Then, in the second step, the switching states computed by the MPC-based algorithm were applied to the three-phase converter. Fig.7 shows the response of the dc-link voltage V_{dc} after switching signals application. It can be noted that V_{dc} voltage reaches its reference with zero error during steady state operation.

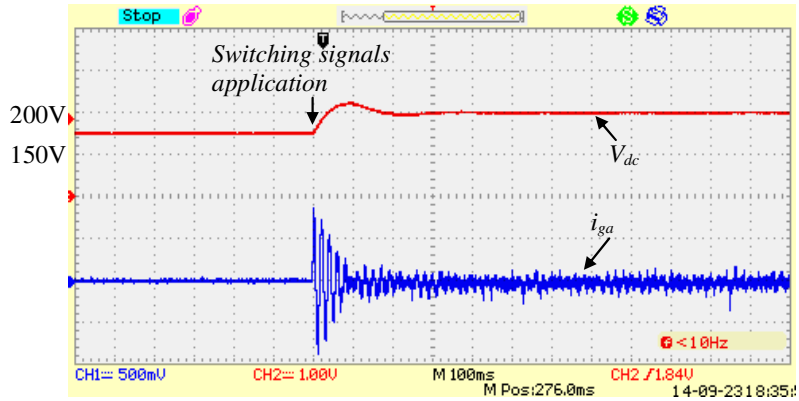

Fig.7. dc-link voltage V_{dc} (100V/Div) and grid current i_{ga} (1.5A/Div) responses at the start-up of the MPC-based control algorithm

Finally in the third step, a load is connected to the dc-link. Fig.8 shows the dc-link voltage V_{dc} and the grid current i_{ga} waveforms.

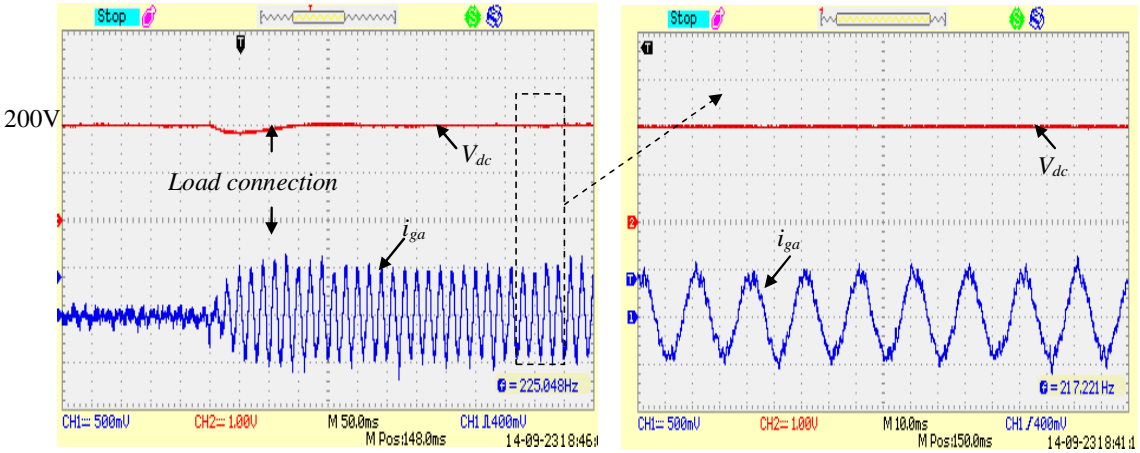

Fig.8. dc-link voltage V_{dc} (100V/Div) and grid current i_{ga} (1.5A/Div) waveforms after the load connection and during steady state operation

As depicted in this figure, the dc-link voltage V_{dc} decreases slightly due to a sudden connection of the load, then the PI-based controller compensates the load disturbance and the V_{dc} voltage remains equal to its reference V_{dc}^{*}. It can be noted also that the grid current increases with sinusoidal waveform after the load connection.

Fig.9 shows the waveform of the grid voltage V_{ga} with regard to the grid current i_{ga} and grid voltage position θ_{dq} during steady state operation. It can be noted that the three phase PWM boost rectifier operates at unity power factor with sinusoidal current absorption. The obtained THD value is equal to 12.10%.

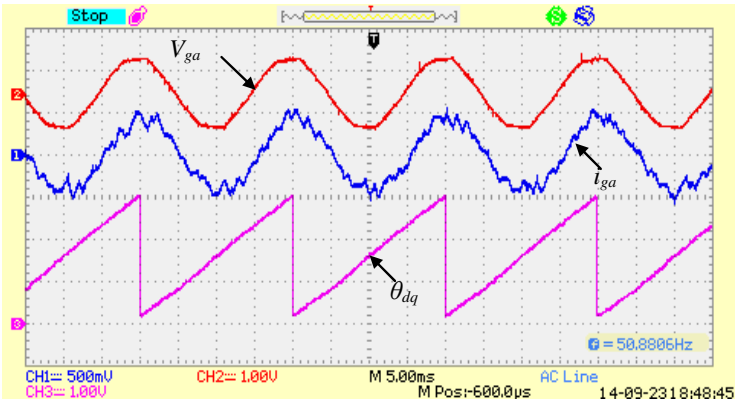

Fig.9. Grid voltage V_{ga} (100V/Div), grid current i_{ga} (1.5A/Div) and grid voltage position θ_{dq}.

5. Conclusion

A Model based Predictive Control (MPC) for three-phase grid-connected converter in wind power systems has been presented. The control was divided into two control loops: the external one control the dc-link voltage V_{dc} and is based on a PI controller while the second one focuses on the control of the grid current and is based on the MPC algorithm. In each sampling period, the proposed strategy calculates the converter switching time, which minimizes the cost function defined as a sum of the absolute values of the current errors. The used control strategy is validated through simulation and experimental tests. The obtained results gave proof of the effectiveness and the performances of the implemented MPC based algorithm especially low harmonic distorted grid current waveforms.

APPENDIX

Table3: Parameters of Three-phases grid connected converter

Parameter	Value	Description
C	1100uF/800V	dc-link capacitor
L_g	50mH/20A	Filter inductance
R_g	3 Ω	Filter resistance
R_{load}	250 Ω	Load resistance
T_s	125µs	Sampling period
T_{ex}	114 µs	Execution time

Acknowledgment

This work was supported by the Tunisian Ministry of High Education and Research under Grant LSE-ENIT-LR11ES15.

The notation used throughout the paper is stated below.

Nomenclature

L	Inductance
R	Resistance
V_g	Grid voltage

i_g	Grid current
V_{dc}	dc-link voltage
θ_{dq}	Grid voltage position
ω_g	Angular frequency of the grid voltage
V_{conv}	Converter output voltage
a,b,c	Stationary reference frame index
A,β	Stationary coordinates
d,q	Synchronous reference frame index
P	Active power
Q	Reactive power
D	Distorted power
g	Cost function
S	Switching states
T_s	Sampling period
T_{ex}	Execution time
THD	Total harmonic distortion
PLL	Phase Locked Loop
FPU	Floating Point Unit
MPC	Model based Predictive Control
DPC	Direct Power Control
SVM	Space Vector Modulation
ISR	Interrupt Service Routine

References

[1] Z. Song, C.Xia and T.Liu, Predictive Current Control of Three-Phase Grid-Connected Converters with Constant Switching Frequency for Wind Energy Systems, *IEEE Transacstions on Industrial Electronics*, vol. 60, no. 6, June 2013.

[2] H. Bekka, S.Taraft,D.Rekioua,S.Bacha, Power Control Of A Wind Generator Connected To The Grid In Front Of Strong Winds, *J. Electrical Systems* ,267-278, Mars 2013.

[3] F.Blaabjerg and K.Ma, Future on Power Electronics for Wind Turbine Systems, *IEEE Journal of Emerging And Selected Topics In Power Electronics*, Vol. 1, No. 3, September 2013.

[4] M. Schweizer, T. Friedli, and J. W. Kolar, Comparative evaluation of advanced three-phase three-level inverter/converter topologies against two-level systems, *IEEE Transactions on industrial electronics*, vol. 60, no. 12, pp.5515–5527, 2013.

[5] F. Blaabjerg, R. Teodorescu, M. Liserre, and A. V. Timbus, Overview of control and grid synchronization for distributed power generation systems, *IEEE Trans. Ind. Electron*., vol. 53, no. 5, pp. 1398–1409,2006.

[6] J. He, Y. W. Li, and M. S. Munir, A flexible harmonic control approach through voltage-controlled DG-grid interfacing converters, *IEEE Transactions on industrial electronics*, vol. 59, no. 1, pp. 444–455, January. 2012.

[7] Y. A. I. Mohamed, Mitigation of dynamic, unbalanced, andharmonic voltage disturbances using grid-connected inverters with LCL filter, *IEEE Transactions on industrial electronics*, vol. 58, no. 9, pp. 3914–3924, Septembre. 2011.

[8] S. Lee , J-H. Lee , H. Cha , Grid synchronization PLL robust to frequency variation, unbalanced and distorted voltage, *IEEE Energy Conversion Congress and Exposition (ECCE),* 1150 - 1155 ,2011.

[9] M. P. Kazmierkowski, R. Krishnan, and F. Blaabjerg, Control in Power Electronics. *Academic Press - USA*, 2002.

[10] M. Malinowski and M. P. Kazmierkowski, Simple direct power control of threephase pwm rectifier using space vector modulation - a comparative study, *EPE Journal*, vol. 13, no. 2, pp. 28–34, Sept 2003.

[11] A.Chaoui, G-P.Gaubert, A.Bouafia, Direct Power Control Switching Table Concept and Analysis for Three-phase Shunt Active Power Filter, *J.Electrical Systems* , vol 9.1, pp.52-65, 2013.

[12] M. Malinowski, M. Jasinski, and M. P. Kazmierkowski, Simple direct power control of three-phase pwm rectifier using space-vector modulation (dpc-svm), *IEEE Transactions on Industrial Electronics*, vol. 51, no. 2, pp. 447–454, April 2004.

[13] S. Vasquez, J.I. Leon, L.G. Franquelo, J.Rodriguez, H.A. Young, A.Marquez and P.a.Zanchetta, Model Predictive Control, *IEEE Transactions on industrial electronics*, vol. 8, no. 1, pp. 16–31, Mars. 2014.

[14] P. karamanakos, T. Geyer, N. oikonomou, F.D. Kieferndorf and S.Manias, Direct Model Predictive Control, *IEEE Transactions on Industrial Electronics*, vol. 8, no. 1, pp. 32–43, Mars. 2014.

[15] P. Cortes, J. Rodriguez, D. E. Quevedo, and C. Silva, Predictive current control strategy with imposed load current spectrum, *IEEE Transactions Power Electron*., vol. 23, no. 2, pp. 612–618, Mar. 2008.

[16] S. Kouro, P. Cortés, R. Vargas, U. Ammann, and J. Rodríguez, Model predictive control—A simple and powerful method to control power converters, *IEEE Transactions on industrial electronics*, vol. 56, no. 6, pp. 1826–1838, June 2009.

[17] R.O. Ram´ırez, J.R. Espinoza, P.E. Mel´ın, M. E. Reyes, E.E. Espinosa, C.Silva, and E.Maurelia, Predictive Controller for a Three-Phase/Single-Phase Voltage Source Converter Cell, *IEEE Transaction on indusrial informatics*. vol. 10, no. 3, August 2014.

[18] A. Hemdani, M. Dagbagi, M.W. Naouar, L. Idkhajine,I. Slama Belkhodja, E. Monmasson, Indirect sliding mode power control for three phase grid connected power converter, *IET Power Electronics*, Vol. 8, Iss. 6, pp. 977–985, Novembre 2015.

[19] P. karamanakos, T. Geyer, N. oikonomou, F.D. Kieferndorf and S.Manias, Direct Model Predictive Control, *IEEE Trans. Ind. Electron.,* vol. 8, no. 1, pp. 32–43, Mars. 2014.

[20] M.W Naouar, A.A Naassani, E.Monmasson, and I.Slama-Belkhodja, FPGA-Based Predictive Current Controller for SynchronousMachine Speed Drive, *IEEE Transactions on power electronics*, vol. 23, no. 4, July 2008.

[21] R.O. Ram´ırez, J.R. Espinoza, P.E. Mel´ın, M. E. Reyes, E.E. Espinosa, C.Silva, and E.Maurelia, Predictive Controller for a Three-Phase/Single-Phase Voltage Source Converter Cell*, IEEE Trans. on ind. informatics.* vol. 10, no. 3, August 2014.

[22] V.Yaramasu and B.Wu, Predictive Control of a Three-Level Boost Converter and an NPC Inverter for High-Power PMSG-Based Medium Voltage Wind Energy ConversionSystems, *IEEE Trans. On P. electronics*, vol.29, no.10, Oct 2014.

[23] L.Tong, X.Zou, S.Feng, Y.Chen, Y.Kang, Q.Huang and Y.Huang, An SRF-PLL-Based Sensorless Vector Control Using the Predictive Deadbeat Algorithm for the Direct-Driven Permanent Magnet Synchronous Generator, *IEEE Trans. On P. electronics*, vol.29, no.6, Jun 2014.

[24] L.Tarisciotti, P.Zanchetta, A. Watson, S. Bifaretti, and Jon C. Clare, Modulated Model Predictive Control for a Seven-Level Cascaded H-Bridge Back-to-Back Converter, *IEEE Transactions on industrial electronics*, vol. 61, no. 10, October 2014.